行政院國家科學委員會專題研究計畫 期中進度報告

利用水下滑翔機群的海洋行動監測網路技術研發--子計畫一：海洋行動監測網路水下滑翔機群協同式控制系統之研究(2/3)

期中進度報告(精簡版)

計 畫 類 別 ：整合型
計 畫 編 號 ：NSC 95-2221-E-002-410-
執 行 期 間 ：95 年 08 月 01 日至 96 年 07 月 31 日
執 行 單 位 ：國立臺灣大學工程科學及海洋工程學系暨研究所

計 畫 主 持 人 ：郭振華
共 同 主 持 人 ：鄭勝文

處 理 方 式 ：期中報告不提供公開查詢

中 華 民 國 96 年 06 月 20 日

行政院國家科學委員會專題研究計畫期中成果報告

海洋行動監測網路水下滑翔機群協同式控制系統之研究(2/3)

Cooperative Control System for a Group of Underwater Gliders in an Ocean Mobil Sensor Network (2/3)

計畫編號：NSC 95-2221-E-002-410
執行期限：95 年 8 月 1 日至 96 年 7 月 31 日

主持人：郭振華
國立臺灣大學工程科學及海洋工程學系

Abstract -- To improve the performance of a glider in the shallow water operations, we will develop methods to improve the transient behavior of gliders. The accuracy of parameters in a vehicle's dynamic model strongly affects the dynamic performance of its control system. An optimal input design technique for vehicle parameter estimation is presented in this study. The idea is the combination of a dynamic programming method with a gradient algorithm for the optimal input synthesis. Motion data were analyzed with a least-squares technique so that values of parameters could be estimated. The estimated values are compared with arbitrary input signals that are used in system identification. This algorithm for selecting optimal inputs is found to be efficient and robust to noises. This work validated the analysis used to develop the optimal input design, and demonstrated the feasibility and practical utility of the optimal input design technique. This report is the mid-term report of the second year.

Keywords: underwater gliders, ocean observation network, underwater vehicles

摘要

正確的重要運動方程式參數為水下滑翔機運動路徑推算及自動控制之必備條件。本報告提出一個用來鑑定水下滑翔機系統參數的模式，藉由一組最佳化輸入函數，控制本計畫所發展的具前後浮力引擎之水下滑翔機，以鑑定出其運動方程式之參數。此報告為第二年之期中報告，內容包含方程式介紹、鑑定方法、以及參數鑑定之主要結果。

關鍵詞：水下滑翔機、海洋觀測網路、水下載具

1. Mathematical Model

Dynamic system models are often used in system and control architectures, to enhance the system performance. Identification of system parameters is a well-studied problem. Various effective algebraic and numerical solution techniques have been developed to solve for unknown parameters using dynamic system models [1], [2], [3]. These include techniques based on pseudo-inverses, sliding mode observers, Kalman observers, and others. Kim et al. [4] estimated the hydrodynamic coefficients based on two nonlinear observers, the SMO (Sliding Mode Observer) and the EKF (Extended Kalman Filter). Liu [5] discuss about the estimation of surge motion model of ship and using identification technique to derive the model's unknown hydrodynamic coefficients. However, the accuracy/quality of the identified system parameters is a function of both the excitation imposed on the system as well as the measurement noise (sensor noise). The importance of input selection for system identification has been recognized for a long time. Mehra et al. [6] considers the design of optimal inputs for identifying parameters in linear dynamic systems. The criterion used for optimization is the sensitivity of the system output to the unknown parameters as expressed by the weighted trace of the Fisher information matrix. Morelli et al. [7], [8] considered the design of optimal inputs for airplane's linear model equations form the point of view of Cramér-Rao lower bound and its inverse, the Fisher information matrix. Numerical simulations of three types of sea trials are performed to obtain the sensitivities of motions to hydrodynamic coefficients [9]. Jauberthie et al. [10] presented the design of optimal inputs for aircraft nonlinear controlled dynamic models. Graver et al. [11] described the development of feedback control for autonomous underwater gliders, and derived a nonlinear dynamic model of a nominal glider complete with hydrodynamic forces and coupling between the vehicle and the movable internal mass. Also, Graver et al. [12] identified the model parameters to match the steady glides in new flight test data from the SLOCUM glider.Graver [11] model the underwater glider as a rigid body with fixed wings and tail immersed in a fluid with buoyancy control and controlled internal moving mass. We assign a coordinate frame fixed on the vehicle body to have its origin at the CB and its axes aligned with the principle axes of the ellipsoid. Body axes are illustrated in Fig.1. The different masses and position vectors are illustrated in Fig. 2. $r_P = (r_{P1}, r_{P2}, r_{P3})^T$ denotes the position vector of movable mass. Here the m_h is the uniformly distributed hull mass, m_w is point mass for nonuniform hull mass distribution, and r_w is the position vector from CB to m_w. m_b is the variable mass located at CB. $\bar{m}$ is the movable point mass. The total mass of the glider is $m_v = m_h + m_w + m_b + \bar{m}$.

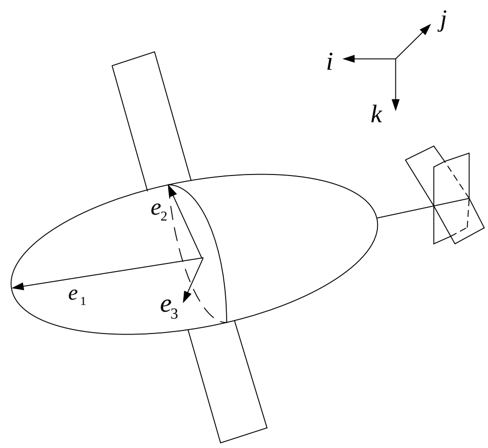

Fig. 1 Frame assignment on underwater glider

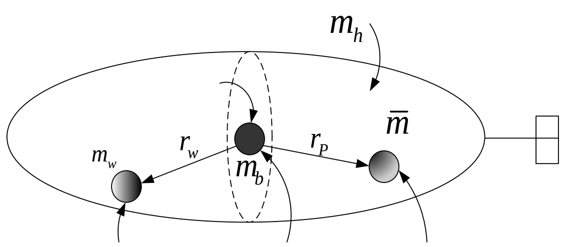

Fig. 2 Glider mass definitions

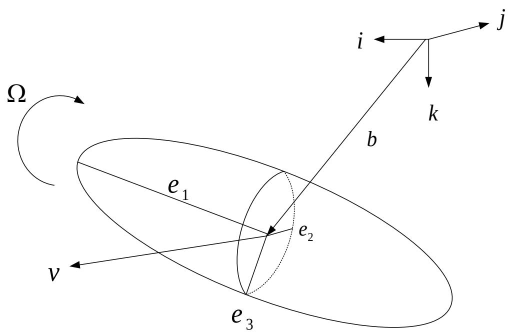

Fig. 3 Glider position and orientation variables

The position of the glider $b = (x, y, z)^T$ is the vector from the origin of the inertial frame to the origin of body frame as shown in Fig. 3. The vehicle moves through the fluid with translational velocity

$v = (v_1, v_2, v_3)^T$ and angular velocity $\Omega = (\Omega_1, \Omega_2, \Omega_3)^T$, expressed with respect to the body frame. In this section, we present a mathematical model that describes the longitudinal dynamics of underwater gliders. Following the discussions in Graver [11], the equations of motion for the gliding vehicle restricted to the vertical plane are

$$\dot{x} = v_1 \cos\theta + v_3 \sin\theta \tag{1}$$

$$\dot{y} = -v_1 \sin\theta + v_3 \cos\theta \tag{2}$$

$$\dot{\theta} = \Omega_2 \tag{3}$$

$$\begin{aligned}\dot{\Omega}_2 = &\frac{1}{J_2}((m_3 - m_1)v_1 v_3 - \bar{m}g(r_{P1}\cos\theta \\ &+ r_{P3}\sin\theta) + M_{DL} - r_{P3}\dot{P}_{P1} + r_{P1}\dot{P}_{P3})\end{aligned} \tag{4}$$

$$\begin{aligned}\dot{v}_1 = &\frac{1}{m_1}(-m_3 v_3 \Omega_2 - P_{P3}\Omega_2 - m_o g \sin\theta \\ &+ L\sin\alpha - D\cos\alpha - \dot{P}_{P1})\end{aligned} \tag{5}$$

$$\begin{aligned}\dot{v}_3 = &\frac{1}{m_3}(m_1 v_1 \Omega_2 + P_{P1}\Omega_2 \\ &+ m_o g\cos\theta - L\cos\alpha - D\sin\alpha - \dot{P}_{P3})\end{aligned} \tag{6}$$

$$\dot{r}_{P1} = \frac{1}{\bar{m}} P_{P1} - v_1 - r_{P3}\Omega_2 \tag{7}$$

$$\dot{r}_{P3} = \frac{1}{\bar{m}} P_{P3} - v_3 + r_{P1}\Omega_2 \tag{8}$$

where m_1 and m_3 are the sum of body and added mass, along the e_1 and e_3 direction. J_2 is the sum of the inertia of stationary mass and added inertia matrix in $e_1 - e_3$ plane. $m_o g$ presents the weight of the glider. P_{P1} and P_{P3} denote linear momentum in body coordinate along the e_1 and e_3 direction. θ is the pitch angle of glider. Here, α is the angle of attack, D is drag, L is lift and M_{DL} is the viscous moment as shown in Fig. 4. Lift and drag forces are assumed to act at the glider center of buoyancy. These forces and moment are modeled as

$$\begin{aligned} L &= (K_{L0} + K_L\alpha)V^2 \\ D &= (K_{D0} + K_D\alpha^2)V^2 \\ M_{DL} &= (K_{M0} + K_M\alpha)V^2 \end{aligned} \tag{9}$$

where the K s are the hydrodynamic coefficients. The aim for parameter identification is to estimate those constant coefficients.

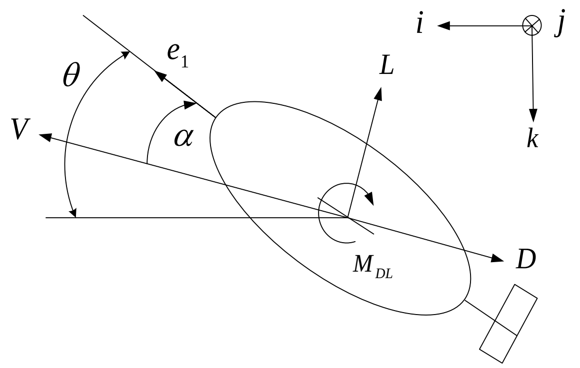

Fig. 4 Lift and Drag on the Glider

As shown in Fig. 4, we denote the glider speed $V = \sqrt{(v_1^2 + v_3^2)}$, and attack angle $\alpha = \tan^{-1}(\frac{v_3}{v_1})$.

2. Identification Results

In this section, simulation results obtained by using the optimal input design algorithm are presented. A glider with fore and aft buoyancy engines was modeled. The conception of the double buoyancy engines is used to replace the moveable mass in Fig. 2 for shifting the center of gravity. Fig. 5 shows the configuration of the buoyancy engines. The mass m_1 =5kg, m_3 =70kg, m_h =40kg, m_o =1kg, $\bar{m}$ =9kg, and internal J_2 =12 kg • m^2 are assumed in the simulation.

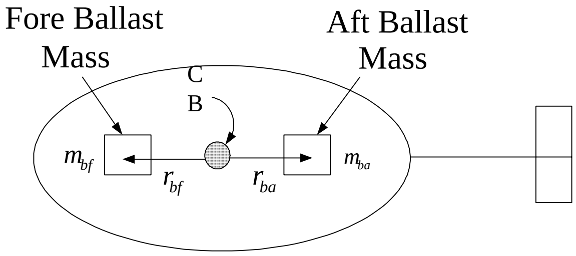

Fig. 5 Fore and Aft Buoyancy Engines

In Fig. 5, m_{bf} and m_{ba} are the mass of ballast mass in the fore and aft buoyancy engines, and r_{bf}, r_{ba} present their position vector from CB. Thus, the variable mass of the glider in Fig. 3.2 becomes

$$m_b = m_{ba} + m_{bf} \tag{10}$$

Here we assume that the variable m_{bf} and m_{ba} used to turn the center of gravity aside are equivalent to move $\bar{m}$ in Fig. 5. In addition, we consider the movable mass is constrained in the longitudinal direction e_1. The equation between this replacement becomes

$$\frac{\bar{m}r_{P1} + m_w r_w}{m_h + m_w + m_b + \bar{m}} = \frac{m_{bf} r_{bf} + m_{ba} r_{ba} + m_w r_w}{m_h + m_w + (m_{ba} + m_{bf}) + \bar{m}} \tag{11}$$

The position vector r_{P1} is then derived as,

$$r_{P1} = \frac{m_{bf} r_{bf} + m_{ba} r_{ba}}{\bar{m}} \tag{12}$$

In Eq. (9), K s are unknown parameters. However, the lift is nearly linear only at low attack angles. Thus the constraint of attack angle was specified by $|\alpha| < 20°$. To make dynamic programming applicable, the simulation experiment is split into stages. In order to avoid a long computational time, the test is split into four stages. At the initial condition, assume the glider is under steady state: the glider speed $V = 0.4$ m/s, the attack angle $\alpha = 1.62°$, the pitch angle $\theta = -27.43°$, the angular velocity $\Omega_2 = 0$.

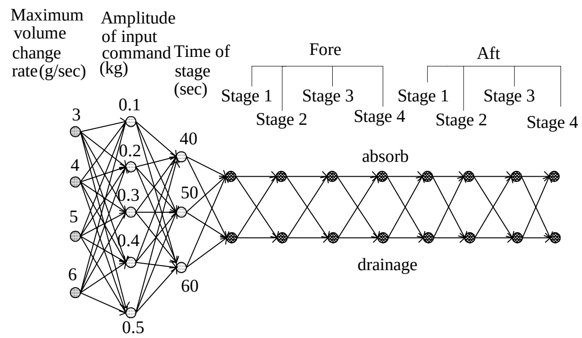

Fig.6 Dynamic Programming Diagram

The simulation variables in this dynamic programming procedure are shown in Fig. 6. All composition of those different variables must be calculated in the optimization process. The variables include the maximum input change rate, the amplitude of square input signal, the time of stage, and the input command choice of absorb or drainage in each stages. Optimal input that makes the cost function minimized can be calculated. The simulation of optimal input is compared with the conventional input. Fig. 7 and Fig. 8 show the optimal input and conventional input signals for the fore and aft buoyancy engines, respectively. This conventional input is used to compare with optimal input, and it is a regular signal which makes the glider ascends and dives, repeatedly. The capacity of each buoyancy engines is assumed 1kg. In these figures, the dash line represents the command input signal and the solid line corresponds to actual input response of the buoyancy engines. The rate of change of the ballast mass is constrained by the buoyancy engine, and this limit is also determined by the dynamic programming principle. It can be seen that the input signals change very slowly and bounded. They could be applied as input signals for real underwater glider system.

Following Eqs. (4)-(6), we can establish the sensitivity differential equation of $(\Omega_2, v_1, v_3)^T$ to hydrodynamic coefficients. Then the output sensitivities were solved from the sensitivity differential equation by Runge-Kutta algorithm of order 4. The quality of the identified parameter can be evaluated by the sensitivity analysis of the observation process. Figs.9-26 compare the sensitivities of square inputs and optimal inputs for the parameters. In these figures, the dash-dot line represents the square inputs and the solid line corresponds to optimal inputs, respectively. Obviously, the output sensitivities to K_D during optimal input have larger variation than conventional input.

To estimate the parameters, Least Squares method is designed using the dynamic model of Eqs. (4) -(6). In these equations, the observations are given by $(\Omega_2,\ v_1,\ v_3)^T$. The hydrodynamic forces and moment in Eqs. (4) -(6) can be written as

$$\begin{bmatrix} L \\ D \\ M_{DL} \end{bmatrix} = \begin{bmatrix} \sin\alpha & -\cos\alpha & 0 \\ \cos\alpha & \sin\alpha & 0 \\ 0 & 0 & 1 \end{bmatrix} \begin{bmatrix} m_1\dot{v}_1 + m_3 v_3\Omega_2 + P_{P3}\Omega_2 + m_o g\sin\theta + \dot{P}_{P1} \\ -m_3\dot{v}_3 + m_1 v_1\Omega_2 + P_{P1}\Omega_2 + m_o g\cos\theta - \dot{P}_{P3} \\ J_2\dot{\Omega}_2 - (m_3 - m_1)v_1 v_3 + \bar{m}g(r_{P1}\cos\theta + r_{P3}\sin\theta) \\ + r_{P3}\dot{P}_{P1} - r_{P1}\dot{P}_{P3} \end{bmatrix} \tag{13}$$

The relation between unknown parameters to L, D and M_{DL} from Eq (9) can also be expressed in matrix form as

$$\begin{bmatrix} V^2 & \alpha V^2 & 0 & 0 & 0 & 0 \\ 0 & 0 & V^2 & \alpha^2 V^2 & 0 & 0 \\ 0 & 0 & 0 & 0 & V^2 & \alpha V^2 \end{bmatrix} \begin{bmatrix} K_{L0} \\ K_L \\ K_{D0} \\ K_D \\ K_{M0} \\ K_M \end{bmatrix} = \begin{bmatrix} L \\ D \\ M_{DL} \end{bmatrix} \tag{14}$$

Substitute Eqs. (14) into Eq (13), a solution of unknown parameters K s can be identified. The estimated and true parameters are compared in Table 1. This result is calculated from 10 times identification in each case. The error and standard error are used to evaluate the quality of identification. In Table 1, it is shown that K_L, K_D have errors larger than other parameters. Due to the output sensitivities to K_D during optimal input are very large, the accuracy of K_D identification in optimal input is better than squae input. At the same time of the sensitivity analysis, a number of states of the glider were also computed from Eqs. (3)-(8). Fig. 27 and Fig. 28 show the time history of attack angle and Euler angles. The trajectory of the glider during optimal input and conventional input for parameter identification in the vertical plane can be calculated from Eqs. (1), (.2), and it was presented in Fig. 29. The measurement states including velocities and angular velocity were plotted in Figs. 30-32. Generally speaking, the time history of sensitivity varies with the output response. The sensitivities of angular velocity to parameters are generally very similar between those two inputs. That is because the time histories of angular velocity in the two cases have little difference in Fig. 30. In addition, due to the terms of K_L, K_D and K_M in Eq (9) increase with attack angle α, the change of attack angle under optimal inputs is more violent than square inputs. The lift in Eq (9) only allows low attack angle. That is the reason why the output sensitivities to K_D are larger than others in the optimal inputs. In a word, although the identified results in Table 1 using optimal inputs only have smaller error to the parameters K_{D0}, K_D, the accuracy of K_D has much higher quality. The standard errors of K_{L0}, K_{D0}, K_D, K_{M0} in optimal input were smaller than the square input.

3. Conclusion

In this report we provide a summary on an optimal input design algorithm developed based on sensitivity analysis for underwater vehicle parameter identification. The main contribution of this work is the design method of optimal input which provides better performance for glider parameter identification. The optimization procedure developed in this work provides optimal inputs by minimizing a cost function. Pulse-like inputs were selected utilizing a dynamic programming technique by evaluating output sensitivities to model parameters. A glider with fore and aft buoyancy engines was modeled. Successful implementations of a least-squares technique on a Slocum glider confirms the applicability of the parameter identification process.

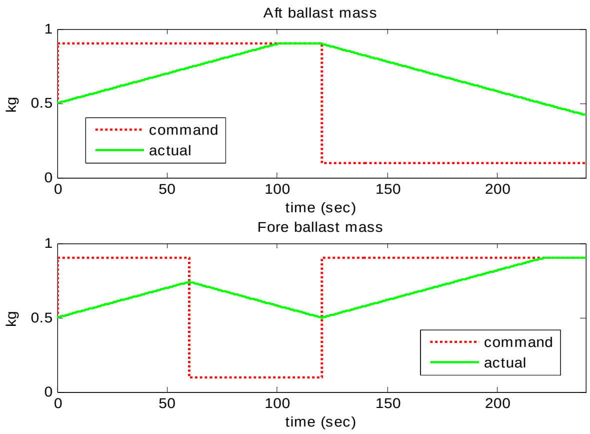

Fig 7 Optimal Inputs of a Glider

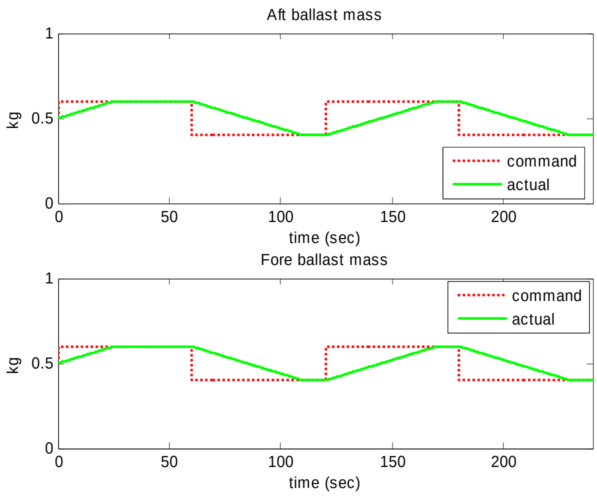

Fig 8 Conventional Inputs of a Glider

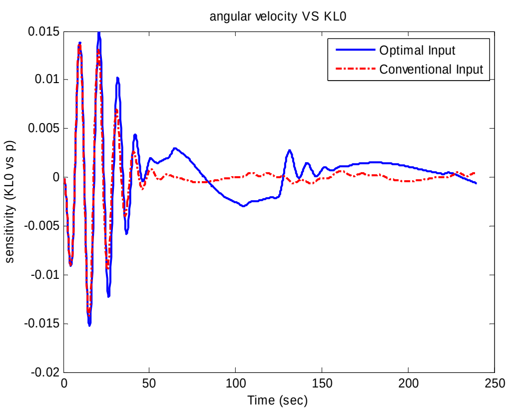

Fig 9 Time history of sensitivity. (K_{L0} to angular velocity Ω)

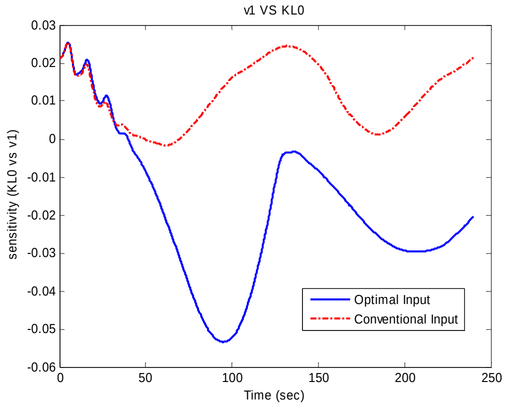

Fig 10 Time history of sensitivity. (K_{L0} to velocity v_1)

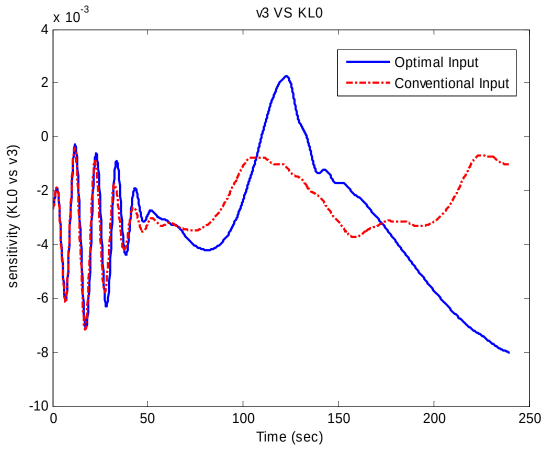

Fig.11 Time history of sensitivity. (K_{L0} to velocity v_3)

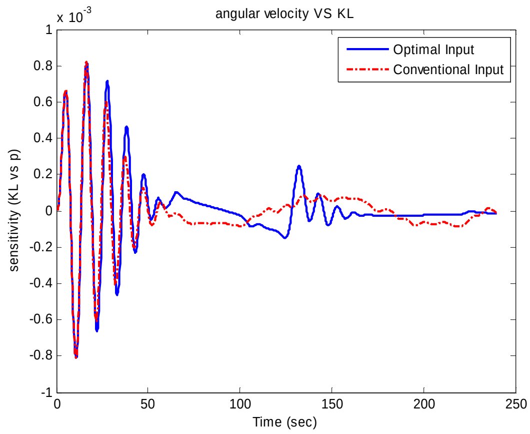

Fig. 12 Time history of sensitivity. (K_L to angular velocity Ω)

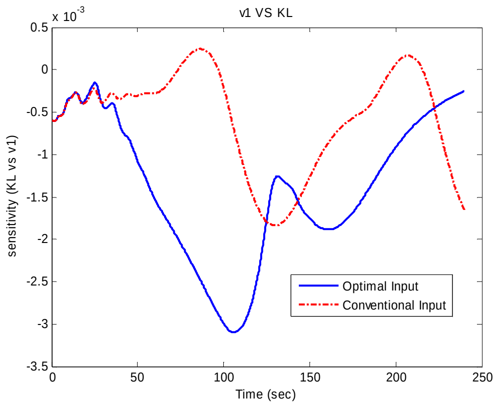

Fig. 13 Time history of sensitivity. (K_L to velocity v_1)

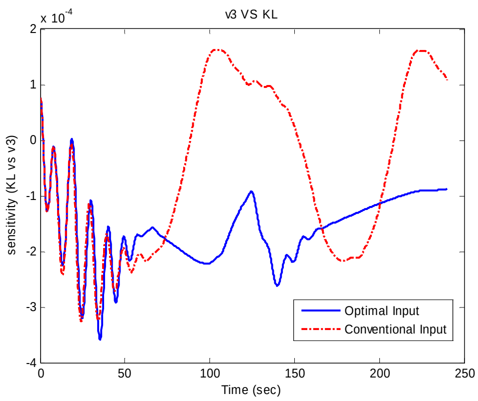

Fig. 14 Time history of sensitivity. (K_L to velocity v_3)

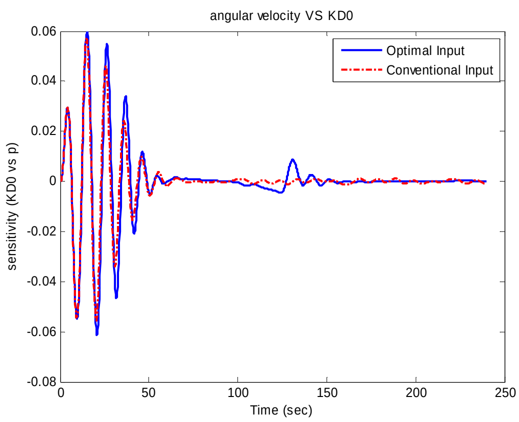

Fig. 15 Time history of sensitivity. (K_{D0} to angular velocity Ω)

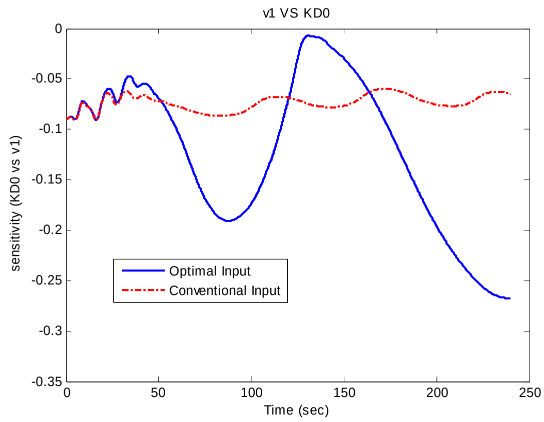

Fig.16 Time history of sensitivity. (K_{D0} to velocity v_1)

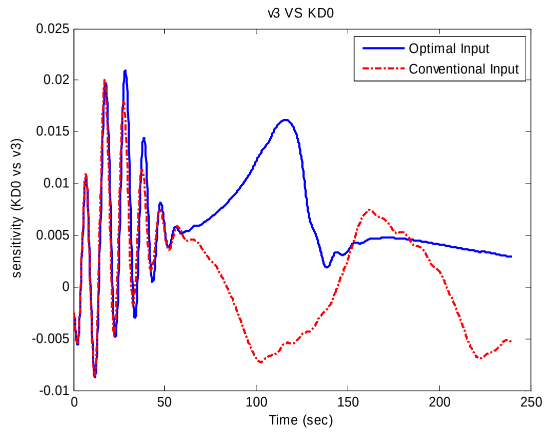

Fig. 17 Time history of sensitivity. (K_{D0} to velocity v_3)

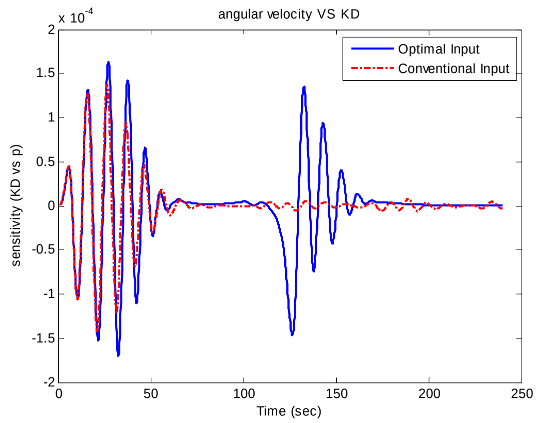

Fig. 18 Time history of sensitivity. (K_D to angular velocity Ω)

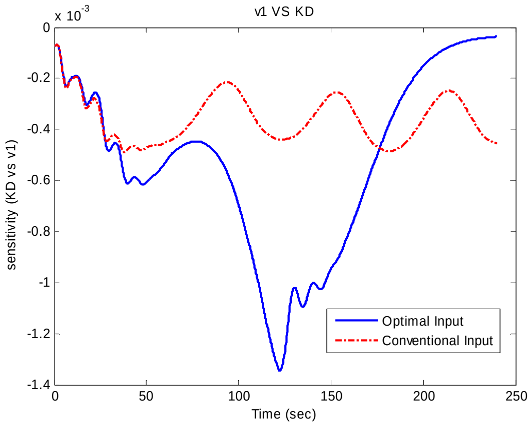

Fig. 19 Time history of sensitivity. (K_D to velocity v_1)

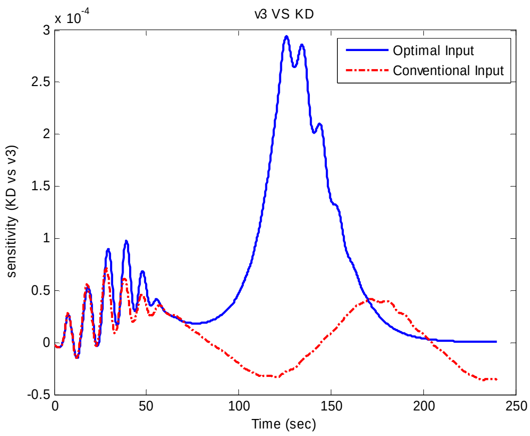

Fig. 20 Time history of sensitivity. (K_D to velocity v_3)

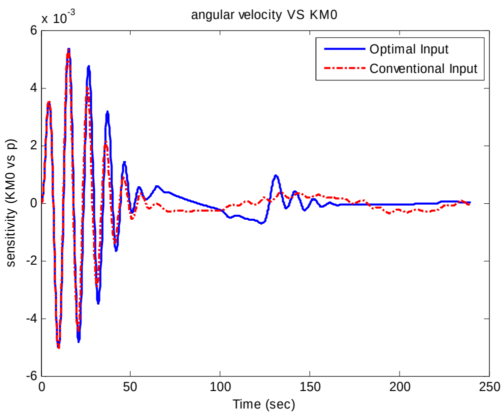

Fig. 21 Time history of sensitivity. (K_{M0} to angular velocity Ω)

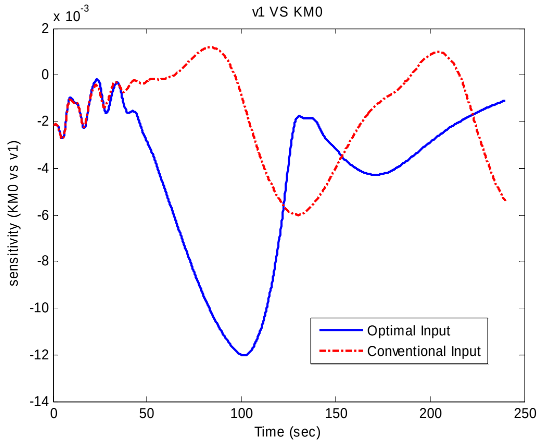

Fig. 22 Time history of sensitivity. (K_{M0} to velocity v_1)

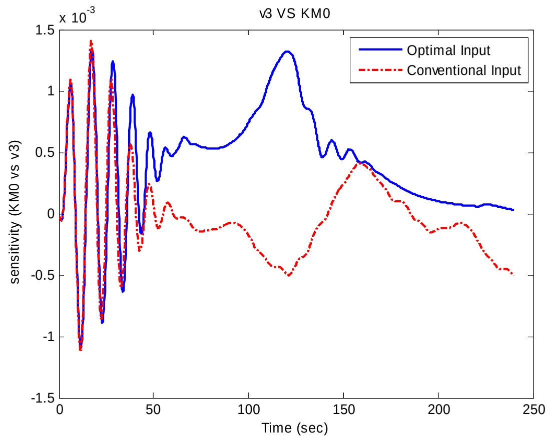

Fig. 23 Time history of sensitivity. (K_{M0} to velocity v_3)

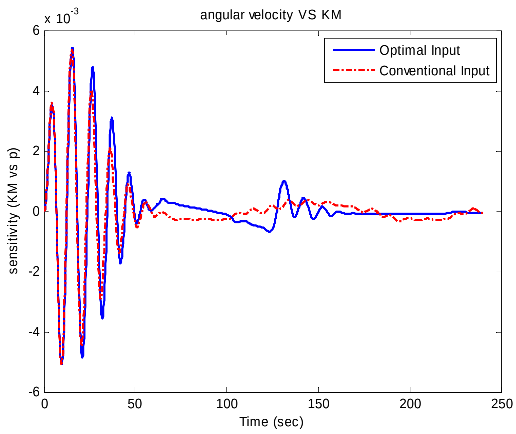

Fig. 24 Time history of sensitivity. (K_M to angular velocity Ω)

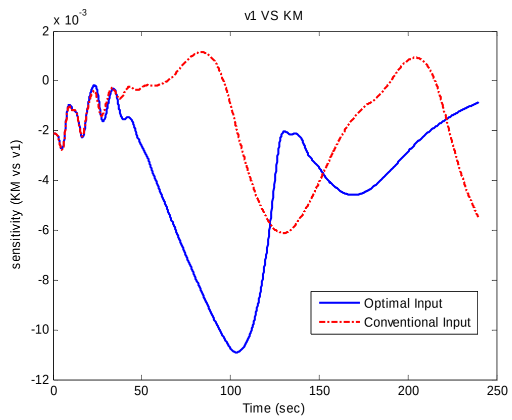

Fig. 25 Time history of sensitivity. (K_M to velocity v_1)

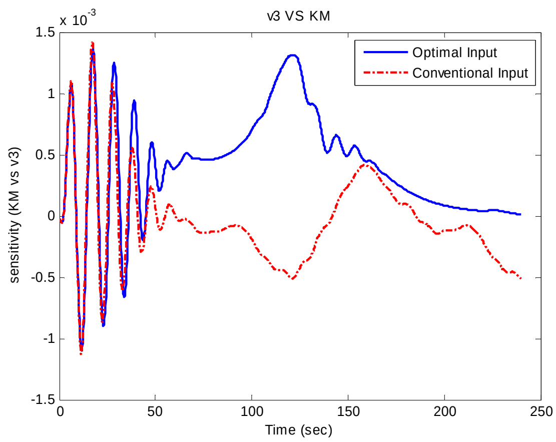

Fig. 26 Time history of sensitivity. (K_M to velocity v_3)

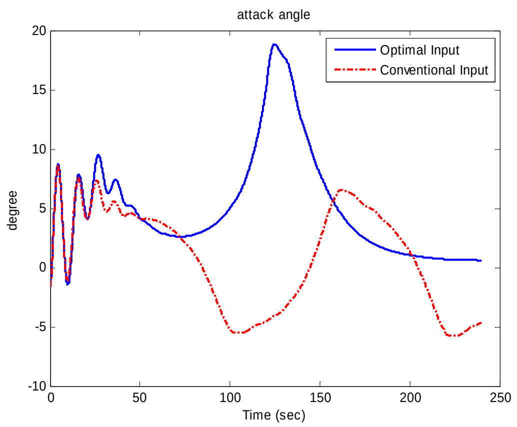

Fig. 27 Time history of attack angle.

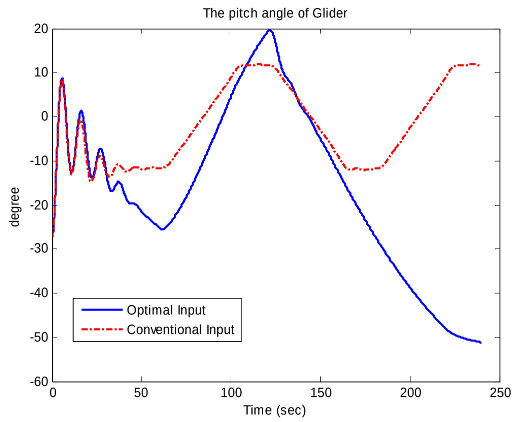

Fig. 28 Time history of Euler angle.

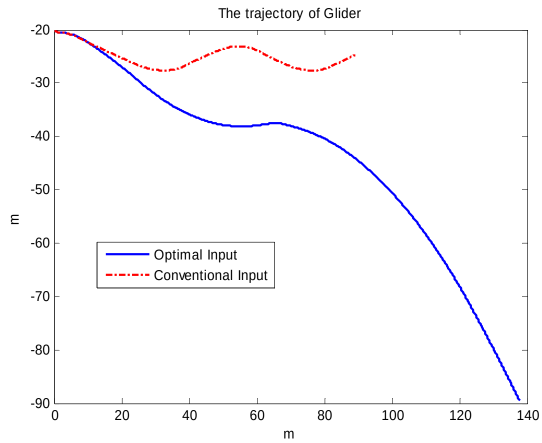

Fig. 29 The 2D Trajectory of the Glider for Parameter Identification.

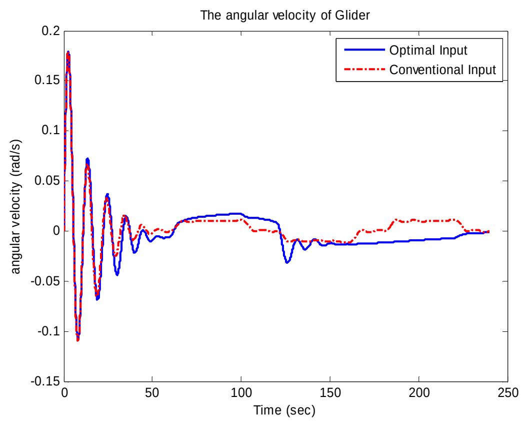

Fig. 30 Time history of angular velocity.

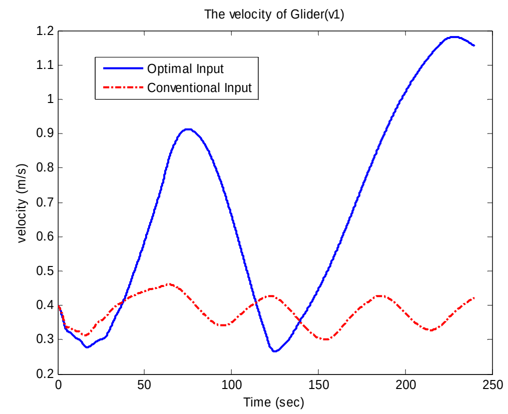

Fig. 31 Time history of velocity (v_1).

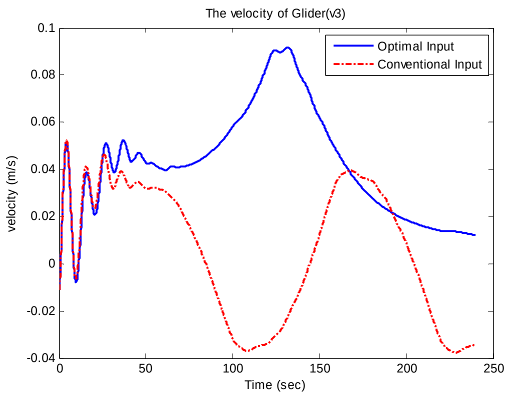

Fig. 32 Time history of velocity (v_3).

References

[1] M. Gautier and P. Poigent, "Extended Kalman Filtering and Weighted Least Squares Dynamic Identification of Robot," Control Engineering Practice, vol. 9, No. 12, pp. 1361-1342, 2001.

[2] L. R. Ray, "Nonlinear Tire Force Estimation and Road Friction Identification: Simulation and Experiment," Automatica, vol. 33, No.10, pp. 1819-1833, 1997.

[3] V. A. Sujan and S. Dubowsky, "An Optimal Information Method for Mobile Manipulator Dynamic Parameter Identification," IEEE/ASME Transactions on Mechatronics, vol. 2, No 2, pp. 215-225, June 2003.

[4] J. Kim, K. Kim, H. S. Choi, W. Seong, and K.-Y. Lee, "Estimation of Hydrodynamic Coefficients for an AUV Using Nonlinear Observers," IEEE Journal of Oceanic Engineering, vol. 27, pp. 830-840, October 2002.

[5] G. Liu, "Application of EKF technique to ship resistance measurement, " Automatica, Vol. 29, No.2, pp. 275-283, 1993.

[6] R. K. Mehra, "Optimal Inputs for Linear System Identification," IEEE Transactions on Automatic Control, vol. AC-19, No.3, pp. 192-200, June 1974.

[7] E. A. Morelli, "Flight Test Validation of Optimal Input Design and Comparison to Conventional Inputs," AIAA paper 97-3711, AIAA Atmospheric Flight Mechanics Conference, New Orleans, Louisiana, August 1997.

[8] E. A. Morelli, "Practical Input Optimization for Aircraft Parameter Estimation Experiments", Sc.D. Dissertation, George Washington University JIAFS, July 1990.

[9] Yeo, Dong Jin, Rhee, Key Pyo, "Sensitivity Analysis of Submersibles' Manoeuvrability and Its Application to the Design of Actuator Inputs." Ocean Engineering, vol. 33, No.17-18, 2006.

[10] C. Jauberthiea, "Optimal Input Design for Aircraft Parameter Estimation", Aerospace Science and Technology, vol. 10, Issue 4, pp. 331-337, 2006.

[11] N. E. Leonard and J. G. Graver, "Model-Based Feedback Control of Autonomous Underwater Gliders", IEEE Journal of oceanic engineering, vol. 26, No. 4, pp. 633-645, October 2001.

[12] J. G. Graver, "Underwater Glider Model Parameter Identification", Proc. 13th Int. Symp. on Unmanned Untethered Submersible Technology (UUST), August 2003.

.

Table 1 Identification for Parameters of a Glider

Parameter	True value	Identification with Optimal Input	Standard Error	Error	Identification with Conventional Input	Standard Error	Error
K_{L0}	0	0.4979	0.001356	0.4979	0.25182	0.000432	0.25182
K_L	132.5	113.57	0.683944	18.93001	117.2841	0.675519	15.21587
K_{D0}	2.15	2.14177	0.00000321	0.00823	2.01355	0.0000835	0.13645
K_D	25	27.95711	0.592654	2.95711	42.56143	2.821345	17.56143
K_{M0}	0	-0.13341	0.0000926	0.13341	-0.07062	0.000215	0.07062
K_M	-100	-94.9997	0.070849	5.00035	-95.8451	0.026218	4.15486
Avg. Error		4.587835			6.231842		
Cost Function		21.0126			87.1188		